Progress in Oceanography 83 (2009) 386–392

Contents lists available at ScienceDirect

Progress in Oceanography

journal homepage: www.elsevier.com/locate/pocean

# Interannual variability in chlorophyll concentrations in the Humboldt and California Current Systems

Andrew C. Thomas *, Peter Brickley, Ryan Weatherbee

*School of Marine Sciences, University of Maine, Orono, ME 04401-5706, USA*

ARTICLE INFO

*Article history:*
Received 10 July 2008
Received in revised form 24 February 2009
Accepted 16 July 2009
Available online 26 July 2009

ABSTRACT

SeaWiFS data provide the first systematic comparison of 10 years (1997–2007) of chlorophyll interannual variability over the California (CCS) and Humboldt (HCS) Current Systems. Dominant signals are adjacent to the coast in the wind-driven upwelling zone. Maximum anomalies in both systems are negative signals during the 1997–1998 El Niño that persist into 1999 at most latitudes. Thereafter, anomalies primarily appear to be associated with shifts in phenology, with those in the CCS stronger than those of the HSC. Prominent signals in the CCS are positive anomalies in 2001–2002 at latitudes >35°N and <30°N, and in 2005–2006 from ~30 to 45°N that persist at latitudes >40°N into 2007. In the HCS, latitudinally extensive positive events occur in austral summers of 2002–2003, 2003–2004. Relationships of chlorophyll anomalies to forcing are explored through correlations to local upwelling anomalies and three indices of Pacific Ocean basin-scale variability, the Multivariate El Niño Index (MEI), the Pacific Decadal Oscillation (PDO) and the North Pacific Gyre Oscillation (NPGO). These show that each system has strong latitudinal regionality in linkage to forcing. At higher latitudes, correlations follow expected relationships of increased (decreased) chlorophyll with positive upwelling and NPGO (MEI and PDO). At specific latitudes, notably the Southern California Bight and off Peru, where circulation and/or chlorophyll phenology differ from canonical EBUS patterns, correlations weaken or oppose those expected. Correlations excluding the El Niño period remain similar in the CCS but substantially changed in the HCS, indicating much stronger domination of El Niño conditions on HCS anomaly relationships over this 10-year period.

© 2009 Elsevier Ltd. All rights reserved.

## 1. Introduction

Elevated chlorophyll concentrations characteristic of the coastal regions of the two Eastern Boundary Upwelling Systems (EBUS) in the Pacific, the California Current System (CCS) and the Humboldt Current System (HBS) are driven by vertical nutrient flux induced by the dominant equatorward alongshore wind stress and resulting offshore Ekman transport (Huyer, 1983). Over the extensive latitudes of both EBUS regions there is varying seasonality in this wind forcing (Bakun and Nelson, 1991; Hill et al., 1998) that, in conjunction with seasonality in light availability, creates latitudinal differences in chlorophyll seasonality (Thomas et al., 2001a; Mackas et al., 2006). Superimposed on this relatively well documented seasonality is strong interannual variability imposed from basin-scale atmosphere–ocean signals, the most prominent of which is the El Niño Southern Oscillation (ENSO). Previous work has quantified the strong changes in chlorophyll patterns associated with El Niño conditions in the CCS (e.g. Fiedler, 1984; Kahru and Mitchell, 2000; Legaard and Thomas, 2006) and in the HCS (e.g. Thomas et al., 2001b; Carr et al., 2002). At least in the CCS, signals emanating from regions poleward of the EBUS also can impose significant interannual variability on the upwelling ecosystem through changes in transport and water mass characteristics (Freeland et al., 2003; Bograd and Lynn, 2003; Thomas et al., 2003). On longer time scales, changes in the magnitude and sign of the Pacific Decadal Oscillation (PDO), an index of basin-scale surface temperature patterns, have ecological ramifications in the North Pacific (e.g. Francis et al., 1998; Hare and Mantua, 2000; Miller et al., 2004). Recently, Di Lorenzo et al. (2008) show that decadal scale variability in salinity, nutrients and chlorophyll in the southern CCS is correlated with a mode of basin-scale variability in sea surface height indicative of gyre circulation they term the North Pacific Gyre Oscillation (NPGO) that has a footprint on the southern hemisphere.

Satellite data provide the ability to systematically compare chlorophyll variability across these EBUS systems, first using Coastal Zone Color Scanner data (Thomas et al., 1994; Hill et al., 1998) and more recently (Thomas et al., 2001a; Mackas et al., 2006) using the significantly improved systematic global coverage of SeaWiFS data. These studies document and compare seasonal variability, its latitudinal pattern, and its generally strong relationship to seasonal wind forcing. Here we use 10 years of SeaWiFS ocean color data to present the first direct, systematic comparison

* Corresponding author. Tel.: +1 207 581 4335.
*E-mail address:* thomas@maine.edu (A.C. Thomas).

0079-6611/$ - see front matter © 2009 Elsevier Ltd. All rights reserved.
doi:10.1016/j.pocean.2009.07.020

of time and space patterns of interannual variability of chlorophyll in the CCS and HCS, first as departures from dominant patterns of seasonality and then as latitude-specific anomalies. We then discuss these patterns by examining linkages between chlorophyll anomalies and (1) local forcing, characterized as anomalies in local wind-driven upwelling and (2) non-local forcing, characterized by basin-scale climate-related signals captured by the Multivariate El Niño Index (MEI), the Pacific Decadal Oscillation (PDO) and the North Pacific Gyre Oscillation (NPGO).

## 2. Data and methods

Ten years (September 1997–August 2007) of daily 4 km SeaWiFS chlorophyll concentration data were composited into monthly means within each year. Climatological months were formed from 10-year averages and monthly anomalies calculated. A coastal area indicative of the upwelling region was sub sampled from the images as the mean concentration over the first 100 km from the coast at every latitude. All chlorophyll calculations were done in log units to produce geometric means (Campbell, 1995) and final results converted back to chlorophyll units for display. The 100 km average produces a systematic chlorophyll metric for latitudinal comparison. Disadvantages include a possibly biased view of total coastal chlorophyll when the shelf and/or upwelling area is either significantly less than 100 km (e.g. northern Chile) or significantly wider (e.g. Peru). Tested averages over (1) 50 km, (2) 200 km cross-shelf distances and (3) normalized to shelf width (500 m contour), changed the mean chlorophyll values at each latitude but did not significantly alter the view of interannual variability, or the correlations to forcing, offered by the 100 km average used here.

An upwelling index based on offshore Ekman transport is used as a metric of local forcing. Gridded, monthly averaged wind stress values of both the ERS and QuikSCAT satellite scatterometer data made available by CERSAT at IFREMER, France are used. QuikSCAT data begin in 1999 and are used for the period 1999–2007. ERS data are used for the SeaWiFS period prior to this (September 1997–1999). Monthly alongshore wind stress was calculated using the mean trend of local coastal angle over ~2° of latitude and an upwelling index of cross-shelf Ekman transport ($m^3\ s^{-1}\ 100\ m^{-1}$ of coastline) was calculated as a function of latitude in each EBUS. The two scatterometers offer slightly different views of surface wind. To reduce this problem, we calculate a monthly climatology separately for each instrument, and then present only monthly upwelling anomalies. The ERS period used to calculate a climatology is the 4.5 years of data 1996–2000 and the QuikSCAT period used is 8 years, 1999–2007.

Three indices of monthly basin-scale Pacific atmosphere–ocean variability are used as metrics of non-local forcing. The Multivariate ENSO Index (MEI) represents variability imposed by ENSO signals emanating from the eastern equatorial region. The Pacific Decadal Oscillation (PDO) tracks the dominant mode of basin-scale surface temperature variability across the North Pacific (north of 20°N). The North Pacific Gyre Oscillation (NPGO) results from the second mode of surface temperature and dynamic height variability in the North Pacific with patterns that focus on the gyre circulation separating the subarctic from the subtropics (Di Lorenzo et al., 2008).

Calculation of statistical significance of correlations between these data requires care to avoid biases introduced by the nature of the 10 years time series. Obvious seasonal correlation in both wind and chlorophyll records is removed by use of the anomalies and the basin-scale indices are non-seasonal. Each anomaly time series was first detrended using a least squares fit linear function to remove unresolved large scale trends. The number of independent values used to calculate degrees of freedom was then adjusted (reduced) to account for autocorrelation within the time series by dividing the actual number of observations by the (detrended) chlorophyll anomaly integral time scale at each latitude (this varied 1.4–3.8 months).

## 3. Results

### 3.1. Dominant space–time patterns and their anomalies

Dominant large scale patterns of chlorophyll variability over the two regions are effectively summarized using an empirical orthogonal function (EOF) decomposition applied separately on each 10-year monthly time series. We briefly describe the seasonality captured by the EOFs and then focus on departures (anomalies) from this seasonality. The first two modes of variability in the CCS (Fig. 1) explain 29% of the total variance. The dominant mode captures the regionally coherent seasonal cycle (solid line), with maxima during boreal summer (May–August, the main upwelling season), and strong minima in boreal winter (November–January). The space pattern associated with this mode has elevated concentrations along the coast and very weak weighting offshore. The width and strength of this coastal maximum is strongest north of 40°N, is narrower and weaker off central California, even weaker and narrower off Baja, and zero or reversed in the Southern California Bight. The second mode captures additional seasonality with two regions of opposite phase, likely reflecting the EOF's view of latitudinal phasing of the seasonal cycle along the coast (Thomas et al., 2001a). Northern CCS regions are largely negative (Fig. 1c). Just north of Cape Blanco, the sign changes and coastal regions equatorward of this are positive, maximum between Capes Blanco and Mendocino, off San Francisco, Point Conception and along Baja. The time series shows this pattern augments the dominant seasonal cycle; southern (positive) regions have peaks in spring–early summer, northern (negative) regions have peaks in late summer–fall, and the pattern is weakest in boreal winter. The first two modes of the HCS EOF decomposition (Fig. 2) capture 19% of the overall variance. As in the CCS, the first mode (12.6% of the variance) isolates the regionally coherent seasonal cycle (solid line), maximum in the main upwelling period, austral summer (December–February) with strong minima in austral winter (May–July). The spatial pattern is maximum all along the coast, strongest and extending furthest from shore in the main upwelling centers off Peru and extending south from central Chile (~33°S). The second mode (5.9% of variance) space pattern (Fig. 2c) divides the region into two at ~25°S. The time series shows the equatorward (positive) region augments the summer maxima seen in Mode 1 with further maxima lasting into the winter (January–July). The poleward (negative) portion, dominated by variability off southern Chile, augments austral spring–early summer (September–December) concentrations.

Visualization of interannual variability within these EOF modes is simplified by removal of the mean annual signal from each of the EOF time series to show anomalies (blue shading, Figs. 1b and d and 2b and d). In the latitudinally coherent seasonal cycle (Mode 1) maximum anomalies in both EBUS systems over the 10-year period are negative during the 1997–1998 El Niño period. Differences in the timing of the arrival of the ENSO signal in each system with respect to season create negative anomalies spread over two upwelling seasons in the CCS (1997 and 1998), but only one in the HCS. Thereafter, the CCS is characterized by stronger anomalies than the HCS. Major events evident in the CCS are (1) strong positive anomalies in late 2001 and throughout the summer of 2002, (2) a sudden shift from strong negative to strong positive anomalies in summer of 2005 and (3) an extended period of positive anomalies in 2006. Larger anomalies in the HCS after the El Niño period are positive events in the summer upwelling seasons of 1999–2000, 2001–2002 and 2005–2006. Mode 2 anomalies are

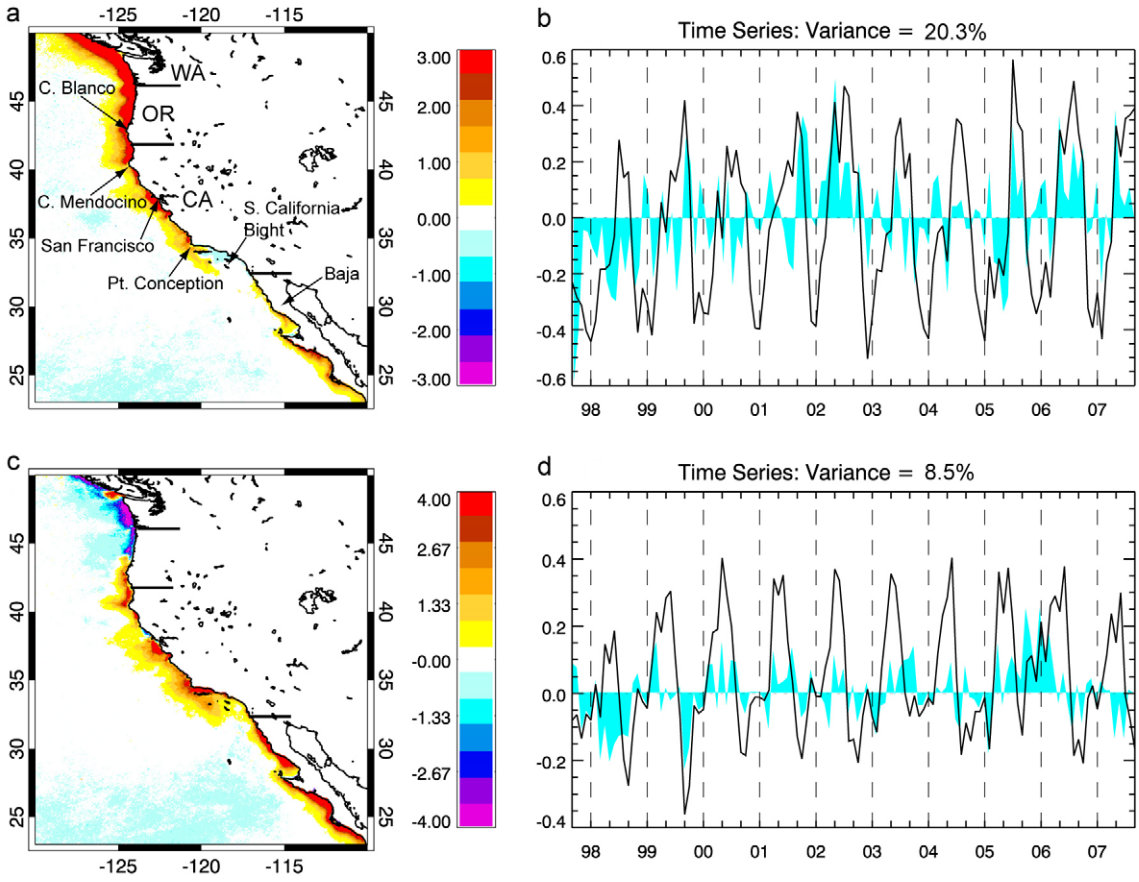


**Fig. 1.** The first (a and b) and second (c and d) modes of an EOF decomposition of monthly SeaWiFS chlorophyll variability in the California Current System over 10 years (1997–2007), showing space patterns, associated time series (solid line) and the% of total variance explained by each. Interannual variability in each mode is highlighted as blue shaded areas of the time series (b and d) showing anomalies of each time series from its 10-year mean annual cycle. Relevant geographic locations are indicated.

more difficult to interpret due to the sign-change in both space and time but they still represent deviations from the 10-year average seasonality captured within the mode. Quantitatively, negative (positive) anomalies in Mode 2 are weaker (stronger) than normal positive time and space signals and stronger (weaker) than normal negative time/space signals. In the CCS, the most obvious deviations from Mode 2 seasonality are (1) the extended negative period in late 1997 and most of 1998 during the El Niño creating weaker concentrations off southern Oregon, California and Baja in this period, (2) a strong negative event in late summer 1999 indicative of elevated fall concentrations off Oregon and Washington and (3) an extended period of positive anomalies in 2005–2006 creating stronger concentrations at lower latitudes. HCS Mode 2 anomalies are dominated by strong negative events in the summers of 1997–1998 and 1998–1999, indicative of weaker chlorophyll in the Peru (positive) region and stronger chlorophyll at higher (negative) latitudes, and positive anomalies in the summers of 2000–2001, 2003–2004 and 2006–2007, creating stronger chlorophyll concentrations off Peru. Outside the ENSO period of 1997–1999, both modes of these EBUS systems suggest that chlorophyll interannual variability is dominated by shifts in phenology.

### 3.2. Chlorophyll anomalies

Although the EOFs isolate regionally coherent dominant patterns, chlorophyll values averaged in the cross-shelf direction over the coastal 100 km at each latitude provide views of actual concentrations, associated anomalies and their spatial location. Monthly mean concentrations within this 100 km region for each EBUS show strong seasonality varying as a function of latitudinal position, similar to that presented by Mackas et al. (2006). The climatological annual cycle at each latitude was subtracted from each year to produce anomalies (Fig. 3a and b). These climatologies (not shown) are qualitatively similar to those based on the first 3 years of SeaWiFS data (Thomas et al., 2001a) and evident in data presented by Mackas et al. (2006).

As expected from the EOFs, strongest (in magnitude, latitudinal extent and duration) anomalies are those during the El Niño period of 1997–1998. In the CCS (Fig. 3a), these are strongest in 1997 north of ~34°N and in 1998 south of 30°N off Baja. In the HCS, strongest anomalies are over the summer of 1997–1998 from Peru into northern Chile (~22°S) and in the upwelling center around 35°S. Strong negative anomalies reoccur off central Peru in both the following summers, but are of shorter duration and less latitudinal extent. These negative anomalies off Peru in the summers following the El Niño are coincident with positive anomalies at higher latitudes (>35°S) off Chile. At the lowest latitudes off northern Peru (<8°S), El Niño anomalies switch to positive by mid 1998.

After the El Niño period, three episodes are the most obvious features in the CCS anomaly data, although others are regionally important. A period of positive anomalies is evident in 2001 and 2002. These begin at mid latitudes (35–45°N) in mid 2001 and become stronger towards the end of the year north of 45°N. These weaken in winter, but are strong north of 40°N throughout 2002 and coincident with strong positive anomalies off Baja. Strong, but relatively short-lived negative anomalies occur in 2005 at higher latitudes and off Baja. Extensive positive anomalies are evident in the final 3 years of data. These begin earliest (2005) off southern California (30–37°N) coincident with the higher latitude negative anomaly. They continue off central California in late

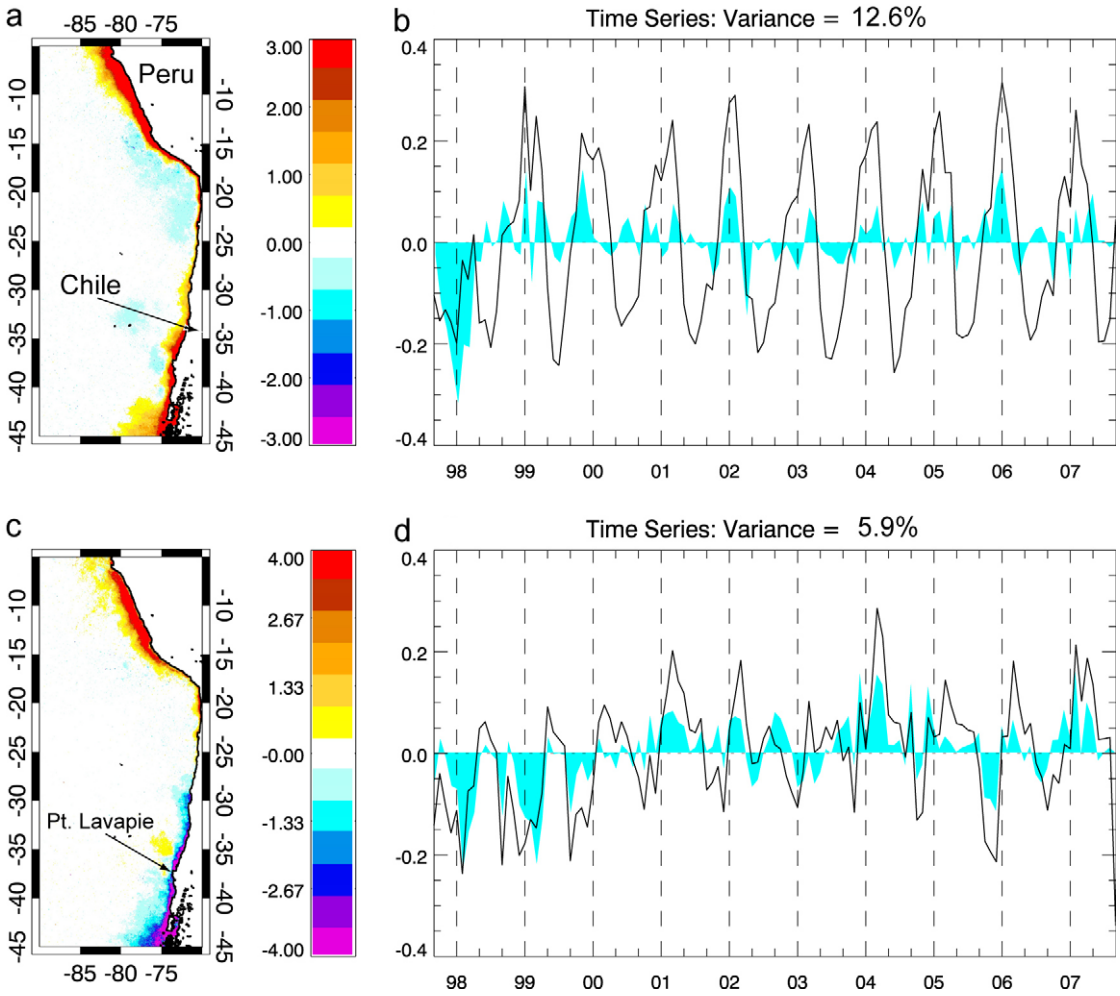


**Fig. 2.** The same as Fig. 1 but for the Humboldt Current System.

2005 and into 2006, centered at ~35°N, and by 2006, positive anomalies dominate. These persist into 2007 at latitudes north of ~42°N. In the HCS, chlorophyll anomalies after the first few years of ENSO perturbation are strongly positive in summer 2001–2002 in a region centered at 35°S, but negative over the rest of the Chilean coast. A latitudinally extensive positive event is present in the summer of 2002–2003 from ~10 to 35°S, and again in 2003–2004 from 5 to 27°S. During both of these episodes, negative anomalies dominate higher latitudes. Summer 2005–2006 has strong positive anomalies off Peru and in all latitudes south of ~30°S. Lastly, 2007 appears to be characterized by strong positive anomalies, especially off Peru early in the year and off Chile south of 35°S at the very end of the record.

### 3.3. Local and basin-scale forcing signals

We characterize local forcing as the coastal wind-driven upwelling intensity. The actual upwelling index (not shown) has strong seasonality that varies as a function of latitude in both EBUS regions, with persistent year-round upwelling dominating at lower latitudes (equatorward of ~32° and 36° in the HCS and CCS, respectively, Mackas et al., 2006) and increasingly strong and prolonged winter downwelling as latitude increases poleward of this. Here we are interested in interannual variability. Anomalies of upwelling as a function of latitude and time (Fig. 3c, d) are characterized by relatively extensive latitudinal coherence, but typically shorter time scales than those of chlorophyll (Fig. 3a, b). In the CCS, anomalies are negative during the early El Niño period, but switch to positive in 1998 and remain so into 1999. Strong positive anomalies are evident north of 35° in 2001 and over the entire CCS in early 2002, switching to negative in late 2002 and into 2003. A strong positive event is evident north of 35°N beginning in the last half of 2004, but this switches to negative over the entire region by early 2005. This negative event weakens (or reverses) in summer 2005, but then becomes negative again by the last quarter to produce negative anomalies that persist into mid 2006. The latter half of 2006 and early 2007 are dominated by strong positive anomalies, especially strong off California (35–40°N). The El Niño period in the HCS (Fig. 3d), in contrast to the CCS, is dominated by strong positive upwelling anomalies. These switch to negative off Peru in late 1998, remaining strongly negative through early 2001. Thereafter, upwelling is strong off Peru though much of 2002 and 2007 and weak in winter–spring of 2006. A region of persistent weak anomalies is evident from ~15 to 25°S, consistent with areas of reduced wind forcing (Hill et al., 1998). At higher latitudes, strong negative anomalies are evident in 2000 and 2002 and over a large latitudinal range in winter–spring 2006. Strong positive anomalies are evident in 1998–1999, and over smaller time–space periods in 2001 and 2003. In 2007, the positive anomalies off Peru extend throughout the latitudinal range of the HCS.

Interannual variability in the three Pacific basin-scale indices over the study period is shown in Fig. 4. The dominant feature in the MEI is the strong 1997–98 El Niño, with a period of negative values during the following La Niña. Thereafter, weaker MEI maxima

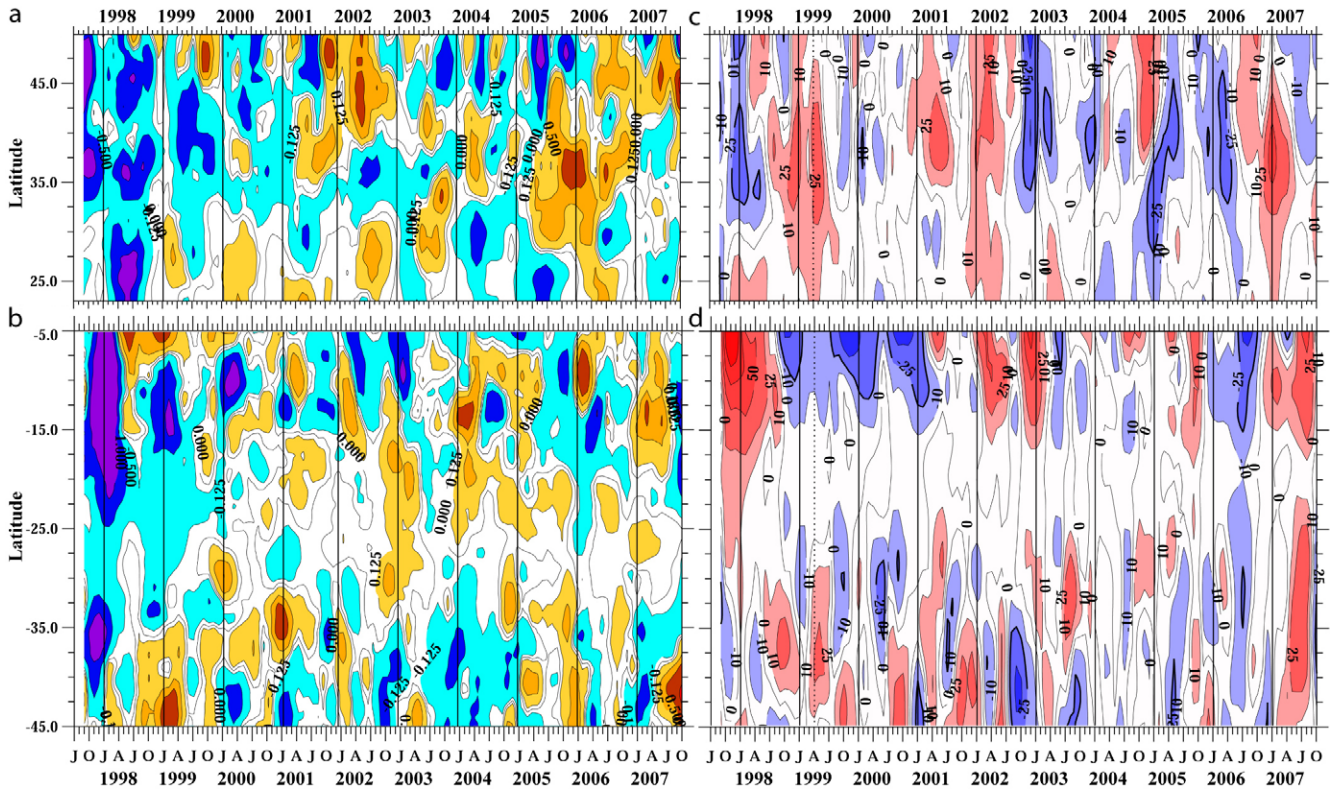


**Fig. 3.** Monthly anomalies of chlorophyll concentration (mg $m^{-3}$) averaged over the 100 km adjacent to the coast plotted as a function of time and latitude over the 10 years study period in the a) CCS and b) HCS (anomalies 0 ± 0.125 mg $m^{-3}$ are white, negative anomalies in blue and positive anomalies in orange) and of scatterometer-derived monthly upwelling index ($m^3$ $s^{-1}$ 100 $m^{-1}$) in the c) CCS and d) HCS (anomalies 0 ± 10 $m^3$ $s^{-1}$ 100 $m^{-1}$ are white, negative anomalies in blue and positive anomalies in red, dotted vertical line in 1999 marks the separation between ERS data and QuikSCAT data.

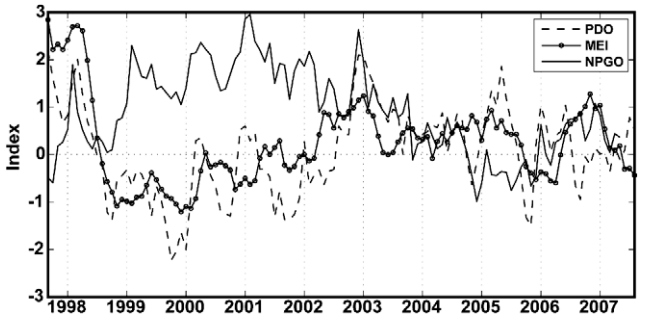


**Fig. 4.** Monthly values of three Pacific basin-scale climate indices over the 1997–2007 study period; the Multivariate El Niño Index (MEI), the Pacific Decadal Oscillation (PDO) and the North Pacific Gyre Oscillation (NPGO).

are present at the ends of 2002 and 2006. The PDO is strongly positive through the El Niño period and then enters a predominantly negative phase in mid 1998 until mid 2002 when it switches to strongly positive. It remains positive (maxima in late 2002 and early 2005), with episodic exceptions until mid 2006, when the signal becomes weaker and variable. The NPGO is weak during the El Niño period, with a single peak exception in February 1998. It becomes strongly positive in early 1999 and remains so until the last part of 2003 when it weakens and becomes negative in late 2004 and through 2005. It switches back to weakly positive in January 2006, remaining predominantly so for the rest of the study period.

## 4. Discussion

The canonical picture of EBUS regions is of increased wind-driven upwelling driving increased phytoplankton production and, therefore, chlorophyll concentrations. Visual comparisons of the upwelling and chlorophyll anomalies (Fig. 3) reveal times and latitudes that both support and contradict this picture. The negative chlorophyll anomalies of the El Niño period are associated with both positive and negative upwelling anomalies in the CCS and strong positive upwelling anomalies through much of the HSC. The latitudinally-coherent positive wind anomalies of 2002 (2007) in the CCS (HCS) are associated with positive chlorophyll anomalies at higher and lower latitudes, but this is not true at mid latitudes. While the negative chlorophyll anomalies at highest latitudes in the CCS in 2005 are coincident with negative wind anomalies, this is not true at mid latitudes where the strong positive chlorophyll anomalies are associated with negative wind anomalies. Off Chile, strong positive chlorophyll anomalies centered at 35°S in summer 2000–2001 are associated with weak positive wind anomalies and extensive positive chlorophyll anomalies in summer 2002–2003 with even weaker upwelling anomalies. Yet at higher latitudes (>35°S) sequences of negative (positive) chlorophyll anomalies in 2001 through 2003 and in the summers of 2005–2006 and 2006–2007 are coincident with negative (positive) upwelling anomalies. Three observations offer some synthesis. First, the El Niño period and associated anomalous subsurface hydrographic structure (e.g. Thomas et al., 2001b; Dever and Winant, 2002) clearly cause relationships between wind-driven upwelling, nutrient flux and phytoplankton response to depart from the simple EBUS canonical picture (Chavez et al., 2002). Second, off Peru, the reversed relationship between upwelling and chlorophyll anomalies evident in Fig. 3 that opposes the canonical picture is consistent with out of phase seasonality of these signals (Thomas et al., 2001a; Echevin et al., 2008). Third, previous work has shown that in EBUS regions, alongshore wind stress and coastal upwelling are not the only relevant wind forcing.

Both wind stress curl and wind mixing influence vertical fluxes and hence the nutrient and light regime experienced by the phytoplankton, neither of which are addressed here (e.g. Abbott and Barksdale, 1991; Halpern, 2002; Henson and Thomas, 2007; Echevin et al., 2008).

The relationship of strong negative chlorophyll anomalies (Fig. 3) in both systems to the positive MEI and PDO (Fig. 4) during the El Niño period is the clearest signal in the time series. Following this, the PDO and MEI (NPGO) enter a negative (positive) phase until 2002. This period coincides with generally negative chlorophyll anomalies at mid latitudes. In 2002 the MEI and PDO switch signs and the NPGO weakens, and this transition period is associated with the first latitudinally widespread positive chlorophyll anomalies to occur in both systems after the El Niño. In the CCS, this period was associated with anomalous equatorward transport of cold, nutrient-rich sub arctic water into the CCS (Freeland et al., 2003) but similar mechanisms have not been shown in the HCS. The weaker and more variable basin-scale indices after 2003 coincide with an increase in occurrence of positive chlorophyll anomalies compared to the beginning of the record, but strong latitudinal variability in the chlorophyll signal makes any synthesis statement difficult.

Systematic relationships between chlorophyll anomalies and forcing are best summarized by statistical comparisons. Correlation between anomalies of upwelling and chlorophyll (Fig. 3) and between chlorophyll anomalies of each latitude and Pacific basin-scale signals (Fig. 4) are plotted as a function of latitude (Fig. 5). Correlations at time lags up to 6 months were examined but are not larger than the zero-lag correlations presented here.

Strong regionality is evident in both the HCS and CCS with regard to linkages between chlorophyll anomalies and the forcing examined here (Fig. 5). Over the 10 year record, chlorophyll anomalies are positively correlated with upwelling anomalies at higher latitudes in the CCS (48 to ~41°N). This correlation disappears between 41 and 31°N. Possible explanations for this are the summer offshore (often >100 km) position of the coastal jet at these latitudes (Strub and James, 2000) which imposes strong control on cross-shelf chlorophyll distributions and hence the 100 km mean viewed here, and the strongly differing circulation and weak (actually reversed) seasonal and relatively weak interannual chlorophyll variability within the Southern California Bight (Fig. 1 and Mackas et al., 2006; Thomas et al., 2001a). The upwelling–chlorophyll correlation becomes significant again off northern Baja (31–27°N), but reverses at the very lowest latitudes where strong solar heating plays a role in stratification, vertical nutrient flux and wind–chlorophyll seasonality (Espinosa-Carreon et al., 2004; Henson and Thomas, 2007). In the HCS, upwelling - chlorophyll correlations are significant and negative off Peru and into northern Chile where wind and chlorophyll phenology are out of phase and mixed layer depth and light play a significant role in surface chlorophyll concentrations (Echevin et al., 2008). Correlations are weakly positive along central Chile and become strongly positive poleward of ~36°S, consistent with expected relationships. In both the CCS and HCS, regions of weak correlation may also be a result of the monthly averages used here and unresolved higher frequency relationships.

A relatively consistent relationship between the basin-scale indices and chlorophyll anomalies is observed as a function of latitude in both EBUS regions. In accordance with canonical models, the correlations of chlorophyll with both the PDO and MEI are negative where they are significant. El Niño events (positive MEI) and the warm (positive) PDO phase are associated with reduced chlorophyll in the upwelling systems. Of interest are the regions where these relationships are not significant. In the CCS, this occurs at ~43–38°N, in the region Capes Blanco and Mendocino and (for the PDO) at ~34°N in the Southern California Bight, both regions

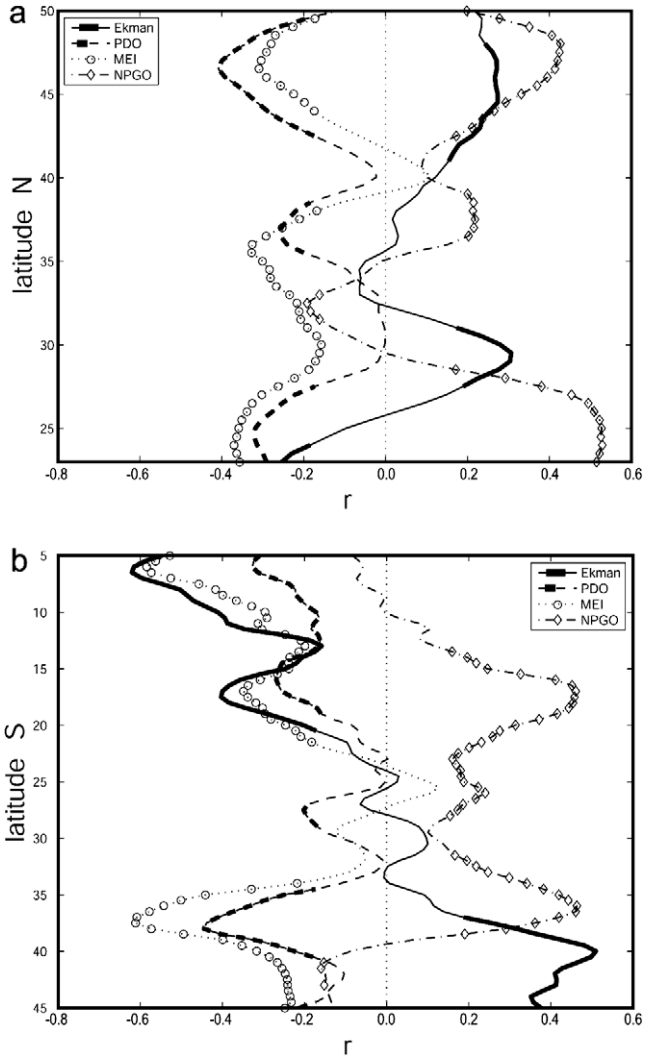


**Fig. 5.** Correlations ($r$ values at zero lag) between monthly chlorophyll anomalies at each latitude and anomalies in upwelling index at each latitude, the Multivariate El Niño Index (MEI), Pacific Decadal Oscillation (PDO) and North Pacific Gyre Oscillation (NPGO), plotted as a function of latitude for a) the CCS and b) the HCS. Bold symbols indicate latitudes where $r$ rises above the 95% significance level.

of recirculation downstream of headlands and strongly reduced 100 km chlorophyll concentrations (Mackas et al., 2006). In the HCS, the relationship weakens off northern Chile, an area where the upwelling region is very narrow and becomes significant again in the wider and stronger upwelling regions south of ~35°S. We note that the surface temperature derived PDO is not completely independent of the MEI. Over the short (10 years) record analyzed here, dominated by the 1997–1999 ENSO event, the two are strongly correlated. The generally positive relationships between chlorophyll anomalies in the CCS and the NPGO are in agreement with the interpretation of the NPGO as indicative of North Pacific gyre circulation and upwelling strength (Di Lorenzo et al., 2008). Correlations weaken in the area of reduced chlorophyll and coastal recirculation at ~40°N, and actually reverse in the Southern California Bight area. In the HCS, relationships of chlorophyll to the NPGO are generally positive except at the very highest latitudes examined (>40°S) where they are negative, and Peru where the NPGO appears to not have a significant footprint. At low latitudes, one explanation is that chlorophyll anomalies in the 10 years record are strongly positively (negatively) related to the MEI (Ekman transport) and these dominate the forcing, but mechanisms behind the high latitude negative correlations are unknown. Lastly, recal-

culating the correlations of Fig. 5 without the first 12 months of data (the El Niño) changes patterns in the CCS very little, suggesting either that chlorophyll–forcing relationships over the 10-year period are similar to those of the El Niño period or that strong anomalies in the later time series do not allow the El Niño to dominate. Such is not true in the HCS where from 10 to 35°S, correlations with upwelling, the PDO and MEI change sign, indicative of strong domination of the 10-year interannual variability in this region by the relationships of the El Niño period.

## 5. Conclusions

Ten years of monthly-averaged satellite chlorophyll data quantify dominant patterns of interannual variability in the CCS and HCS.

- Strongest chlorophyll anomalies in both the CCS and HCS 10 years record are negative anomalies of the 1997–1998 El Niño period. These are associated with both negative and positive wind-driven upwelling anomalies, depending on latitudinal location. Thereafter, anomalies are stronger in the CCS than the HCS and in both systems appear to primarily reflect shifts in phenology.
- Other strong chlorophyll anomalies in the CCS are associated with previously identified anomalous transport events (positive 2001–2002 anomalies) and shifts in wind phenology (2005 anomaly patterns). Such relationships remain less well understood in the HCS, but latitudinally extensive positive anomalies are present in summer 2002–2003 and in 2003–2004.
- Both systems show strong latitudinal regionality in the relationship between chlorophyll anomalies and both local (upwelling) and non-local forcing (MEI, PDO and NPGO). These generally follow expected biological–physical relationships except in regions where differing circulation and/or phenology of wind and/or chlorophyll varies from canonical EBUS patterns (e.g. the Southern California Bight and off Peru).

The actual mechanisms that link this forcing to phytoplankton response, ramifications on higher trophic levels, and details of the relationship between the monthly averages examined here and ecologically important higher frequency variability, await further research.

## Acknowledgements

This work was supported by funding from the US National Science Foundation through Grants OCE 0531289, OCE 0535386, OCE 0814413 and OCE 0815051 to ACT, part of the US GLOBEC program. We thank NASA GSFC for serving the global SeaWiFS data, IFREMER for access to processed scatterometer wind stress data, the University of Washington for the PDO time series, NOAA CDC for access to the MEI and E. DiLorenzo for access to the NPGO time series. This is contribution #616 from the US GLOBEC program.

## References

Abbott, M.R., Barksdale, B., 1991. Phytoplankton pigment patterns and wind forcing off Central California. Journal of Geophysical Research 96, 14649–14667.

Bakun, A., Nelson, C.S., 1991. The seasonal cycle of wind stress curl in subtropical eastern boundary current regions. Journal of Physical Oceanography 21, 1815–1834.

Bograd, S.J., Lynn, R.J., 2003. Anomalous subarctic influence in the southern California Current during 2002. Geophysical Research Letters. doi:10.1029/2003GL017446.

Campbell, J.W., 1995. The lognormal distribution as a model for bio-optical variability in the sea. Journal of Geophysical Research 100, 13237–13254.

Carr, M.E., Strub, P.T., Thomas, A.C., Blanco, J.L., 2002. Evolution of 1996–1999 La Nina and El Nino conditions off the western coast of South America: a remote sensing perspective. Journal of Geophysical Research. doi:10.1029/2001JC001183.

Chavez, F.P., Pennington, J.T., Castro, C.G., Ryan, J.P., Michisaki, R.P., Schlining, B., Walz, P., Buck, K.R., McFadyen, A., Collins, C.A., 2002. Biological and chemical consequences of the 1997–1998 El Nino in central California waters. Progress in Oceanography 54, 205–232.

Dever, E.P., Winant, C.D., 2002. The evolution and depth structure of shelf and slope temperatures and velocities during the 1997–1998 El Nino near Point Conception, California. Progress in Oceanography 54, 77–103.

Di Lorenzo, E., Schneider, N., Cobb, K.M., Chhak, K., Franks, P.J.S., Miller, A.J., McWilliams, J.C., Bograd, S.J., Arango, H., Curchister, E., Powell, T.M., Rivere, P., 2008. North Pacific Gyre Oscillation links ocean climate and ecosystem change. Geophysical Research Letters. doi:10.1029/2007GL032838.

Echevin, V., Aumont, O., Ledesma, J., Flores, G., 2008. The seasonal cycle of surface chlorophyll in the Peruvian upwelling system: a modelling study. Progress in Oceanography 79, 167–176.

Espinosa-Carreon, T.L., Strub, P.T., Beier, E., Ocampo-Torres, F., Gaxiola-Castro, G., 2004. Seasonal and interannual variability of satellite-derived chlorophyll pigment, surface height, and temperature off Baja California. Journal of Geophysical Research 109, C03039. doi:10.1029/2003JC002105.

Fiedler, P.C., 1984. Satellite-Observations of the 1982–1983 El-Nino along the United States Pacific Coast. Science 224, 1251–1254.

Francis, R.C., Hare, S.R., Hollowed, A.B., Wooster, W.S., 1998. Effects of interdecadal climate variability on the oceanic ecosystems of the NE Pacific. Fisheries Oceanography 7, 1–21.

Freeland, H.J., Gatein, G., Huyer, A., Smith, R.L., 2003. Cold halocline in the northern California Current: an invasion of subarctic water. Geophysical Research Letters. doi:10.1029/2002GL016663.

Halpern, D., 2002. Offshore Ekman transport and Ekman pumping off Peru during the 1997–1998 El Nino. Geophysical Research Letters. doi:10.1029/2001GL014097.

Hare, S.R., Mantua, N.J., 2000. Empirical evidence for North Pacific regime shifts in 1977 and 1989. Progress in Oceanography 47, 103–145.

Henson, S.A., Thomas, A.C., 2007. Interannual variability in timing of seasonal chlorophyll increases in the California Current. Journal of Geophysical Research. doi:10.1029/2006JC003960.

Hill, A.E., Hickey, B.M., Shillington, F.A., Strub, P.T., Brink, K.H., Barton, E.D., Thomas, A.C., 1998. Eastern boundary currents: a pan-regional review. In: Robinson, A.R., Brink, K.H. (Eds.), The Sea. J. Wiley and Sons Inc., New York.

Huyer, A.E., 1983. Coastal upwelling in the California Current system. Progress in Oceanography 12, 259–284.

Kahru, M., Mitchell, B.G., 2000. Influence of the 1997–98 El Nino on the surface chlorophyll in the California Current. Geophysical Research Letters 27, 2937–2940.

Legaard, K., Thomas, A.C., 2006. Spatial patterns of seasonal and interannual variability in chlorophyll and surface temperature in the California Current. Journal of Geophysical Research. doi:10.1029/2005JC003282.

Mackas, D., Strub, P.T., Thomas, A.C., Montecino, V., 2006. Eastern ocean boundaries pan-regional view. In: Robinson, A.R., Brink, K.H. (Eds.), The Sea. Harvard Press Ltd., Boston.

Miller, A.J., Chai, F., Chiba, S.E., Moisan, J.R., Neilson, D.J., 2004. Decadal-scale climate and ecosystem interactions in the North Pacific Ocean. Journal of Oceanography 60, 163–188.

Strub, P.T., James, C., 2000. Altimeter-derived variability of surface velocities in the California Current System: 2. Seasonal circulation and eddy statistics. Deep-Sea Research II 47, 831–870.

Thomas, A.C., Huang, F., Strub, P.T., James, C., 1994. Comparison of the seasonal and interannual variability of phytoplankton pigment concentrations in the Peru and California Current Systems. Journal of Geophysical Research 99, 7355–7370.

Thomas, A.C., Blanco, J.L., Carr, M.E., Strub, P.T., Ossus, J., 2001a. Satellite-measured chlorophyll and temperature variability off northern Chile during the 1996–1998 La Nina and El Nino. Journal of Geophysical Research 106, 899–915.

Thomas, A.C., Carr, M.E., Strub, P.T., 2001b. Chlorophyll variability in eastern boundary currents. Geophysical Research Letters 28, 3421–3424.

Thomas, A.C., Strub, P.T., Brickley, P., 2003. Anomalous chlorophyll concentrations in the California Current in 2001–2002. Geophysical Research Letters. doi:10.1029/2003GL017409.